

- Applications of biotransformations and biocatalysis to complexity generation in organic synthesis

Hudlicky, T.; Reed, J. W. *Chem. Soc. Rev.* **2009**, *38*, 3117 – 3132.

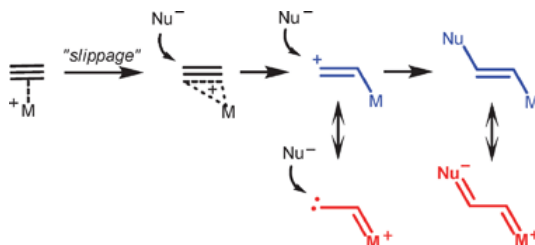
Abstract:



This *tutorial review* provides a survey of syntheses in which an enzymatic step contributed to generating downstream molecular complexity in the target. The first part provides a guide to the types of enzymatic transformations suitable for incorporation into synthetic schemes. The principles of symmetry, especially the concept of “latent symmetry”, which are often used to simplify enantiodivergent design of targets, are discussed next. The examples are discussed in the order of a degree of experimental difficulty associated with the execution of a particular biological technique. Lipase resolutions and desymmetrizations are discussed first followed by more advanced protocols involving oxidoreductase enzymes and ending with examples of syntheses that employ pathway engineering and directed evolution of proteins. Future prospects of biocatalytic methods as means of efficient preparation of target compounds are indicated. The authors hope that the review will serve to convince those synthetic chemists reluctant to use biological methods to include enzymatic procedures in their design.

- Gold and platinum catalysis—a convenient tool for generating molecular complexity  
Fürstner, A. *Chem. Soc. Rev.* **2009**, *38*, 3208 – 3221.

Abstract:

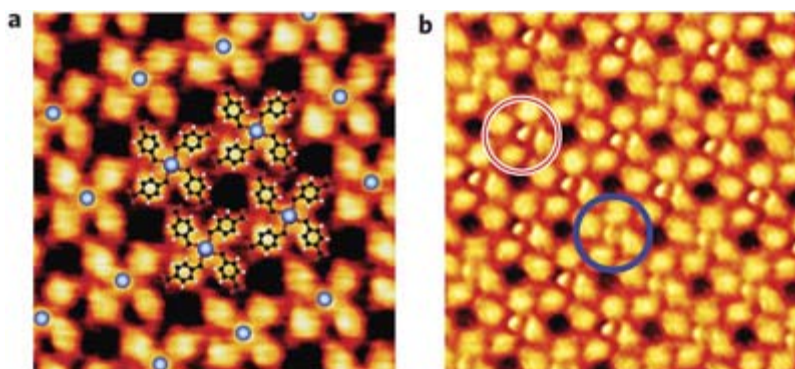


This *critical review* intends to familiarize the reader with the essence of  $\pi$ -acid catalysis, in particular with reactions or reaction cascades effected by gold and platinum complexes. Even though materialized in apparently different reactivity modes, such noble metal catalyzed processes can be easily rationalized on the basis of a uniform mechanistic scheme that is outlined in detail. The resulting increase in molecular complexity is illustrated by selected natural product total syntheses and the formation of various intricate non-natural compounds (106 references).

- Supramolecular control of the magnetic anisotropy in two-dimensional high-spin Fe arrays at a metal interface

Gambardella, P.; Stepanow, S.; Dmitriev, A.; Honolka, J.; de Groot, F. M. F.; Lingenfelder, M.; Gupta, S. S.; Sarma, D. D.; Bencok, P.; Stanescu, S.; Clair, S.; Pons, S.; Lin, N.; Seitsonen, A. P.; Brune, H.; Barth, J. V.; Kern, K. *Nature Materials* **2009**, *8*, 189-193.

Abstract:

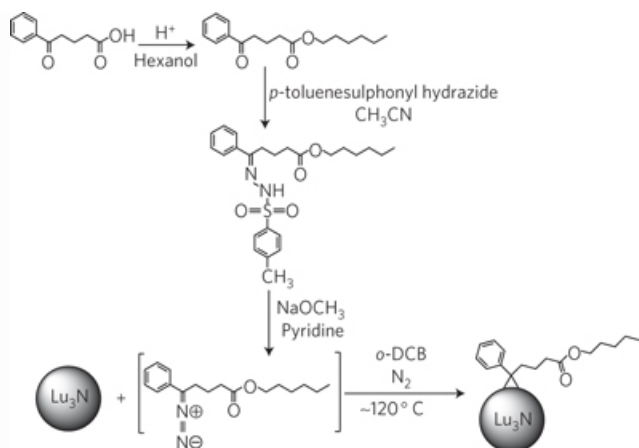


Magnetic atoms at surfaces are a rich model system for solid-state magnetic bits exhibiting either classical or quantum behaviour. Individual atoms, however, are difficult to arrange in regular patterns. Moreover, their magnetic properties are dominated by interaction with the substrate, which, as in the case of Kondo systems, often leads to a decrease or quench of their local magnetic moment. Here, we show that the supramolecular assembly of Fe and 1,4-benzenedicarboxylic acid molecules on a Cu surface results in ordered arrays of high-spin mononuclear Fe centres on a 1.5 nm square grid. Lateral coordination with the molecular ligands yields unsaturated yet stable coordination bonds, which enable chemical modification of the electronic and magnetic properties of the Fe atoms independently from the substrate. The easy magnetization direction of the Fe centres can be switched by oxygen adsorption, thus opening a way to control the magnetic anisotropy in supramolecular layers akin to that used in metallic thin films.

- Endohedral fullerenes for organic photovoltaic devices

Ross, R. B.; Cardona, C. M.; Guldi, D. M.; Sankaranarayanan, S. G.; Reese, M. O.; Kopidakis, N.; Peet, J.; Walker, B.; Bazan, G. C.; Keuren, E. V.; Holloway, B. C.; Drees, M. *Nature Materials* **2009**, *8*, 208-212.

Abstract:



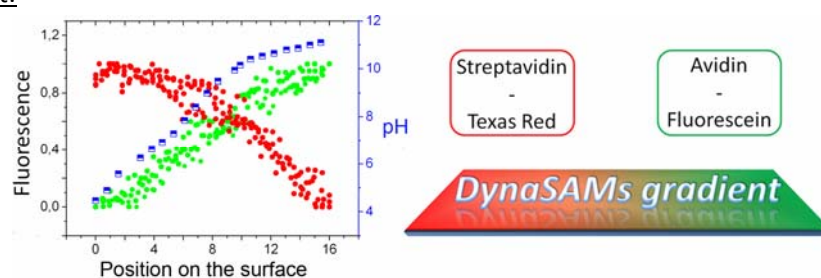
So far, one of the fundamental limitations of organic photovoltaic (OPV) device power conversion efficiencies (PCEs) has been the low voltage output caused by a molecular orbital mismatch between the donor polymer and acceptor molecules. Here, we present a means of addressing the low voltage output by introducing novel trimetallic nitride endohedral fullerenes (TNEFs) as acceptor materials for use in photovoltaic devices. TNEFs were discovered in 1999 by Stevenson *et al.*; for the first time derivatives of the TNEF acceptor,  $\text{Lu}_3\text{N}@C_{80}$ , are synthesized and integrated into OPV devices. The reduced energy offset of the molecular orbitals of  $\text{Lu}_3\text{N}@C_{80}$  to the donor, poly(3-hexyl)thiophene (P3HT), reduces energy losses in the charge transfer process and increases the open circuit voltage

( $V_{oc}$ ) to 260 mV above reference devices made with [6,6]-phenyl-C<sub>61</sub>-butyric methyl ester (C<sub>60</sub>-PCBM) acceptor. PCEs >4% have been observed using P3HT as the donor material. This work clears a path towards higher PCEs in OPV devices by demonstrating that high-yield charge separation can occur with OPV systems that have a reduced donor/acceptor lowest unoccupied molecular orbital energy offset.

- Hierarchical functional gradients of pH-responsive self-assembled monolayers using dynamic covalent chemistry on surfaces

Tauk, L.; Schröder, A. P.; Decher, G.; Giuseppone, N. *Nature Chemistry* **2009**, *1*, 649-656.

Abstract:

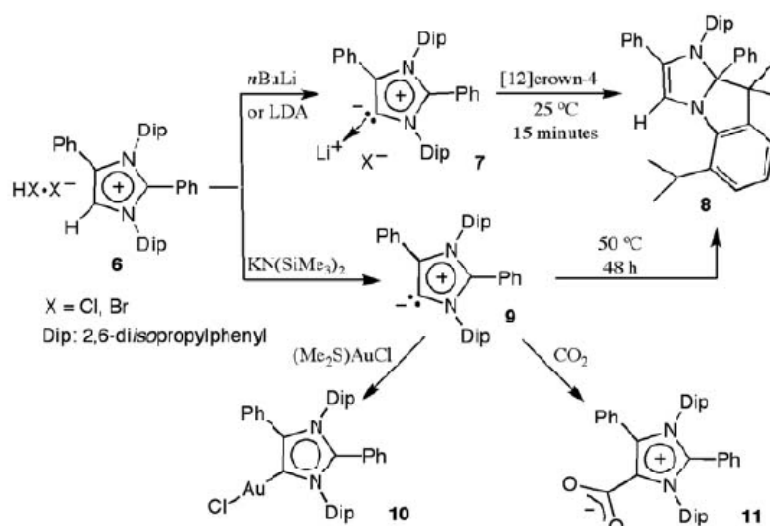


Surface chemistry is an important field of research, especially for the study and design of (bio)nanstructures in which nearly every atom lies at an interface. Here we show that dynamic covalent chemistry is an efficient tool for functionalizing surfaces in such a way that their interfacial properties can be varied controllably in space and time. Modulation of pH is used to tune the fast, selective and reversible attachment of functional amines (with different pK<sub>a</sub> values) to an aldehyde-coated surface. To illustrate the potential of this technique, we developed dynamic self-assembled monolayers ('DynaSAMS'), which enable the hierarchical construction of mixed gradients comprising either small functional molecules or proteins. Control of the (bio)chemical composition at any point on the surface potentially provides a simple bottom-up method to access numerous surface patterns with a broad range of functionalities.

- Isolation of a C5-Deprotonated Imidazolium, a Crystalline "Abnormal" N-Heterocyclic Carbene

Aldeco-Perez, E.; Rosenthal, A. J.; Donnadieu, B.; Parameswaran, P.; Frenking, G.; Bertrand, G. *Science* **2009**, *326*, 556-559.

Abstract:

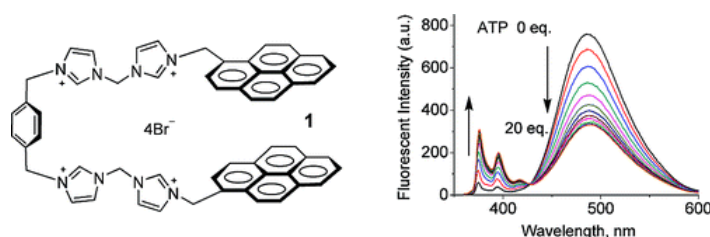


The discovery two decades ago of metal-free stable carbenes, especially imidazol-2-ylidenes [N-heterocyclic carbenes (NHCs)], has led to numerous breakthroughs in organic and organometallic catalysis. More recently, a small range of complexes has been prepared in which alternative NHC isomers, namely imidazol-5-ylidenes (also termed abnormal NHCs or aNHCs, because the carbene center is no longer located between the two nitrogens), coordinate to a transition metal. Here we report the synthesis of a metal-free aNHC that is stable at room temperature, both in the solid state and in solution. Calculations show that the aNHC is more basic than its normal NHC isomer. Because the substituent at the carbon next to the carbene center is a nonbulky phenyl group, a variety of substitution patterns should be tolerated without precluding the isolation of the corresponding aNHC.

- Unique Sandwich Stacking of Pyrene-Adenine-Pyrene for Selective and Ratiometric Fluorescent Sensing of ATP at Physiological pH

Xu, Z.; Singh, N. J.; Lim, J.; Pan, J.; Kim, H. N.; Park, S.; Kim, K. S.; Yoon, J. J. *Am. Chem. Soc.* **2009**, *131*, 15528–15533.

Abstract:



A pincer-like benzene-bridged sensor **1** with a pyrene excimer as a signal source and imidazolium as a phosphate anion receptor was synthesized and investigated for ATP sensing. A unique switch of excimer vs monomer pyrene fluorescence of **1** is observed in the presence of ATP due to the characteristic sandwich  $\pi$ - $\pi$  stacking of pyrene-adenine-pyrene. On the other hand, four other bases of nucleoside triphosphates such as GTP, CTP, UTP, and TTP can interact only from the outside with the already stabilized stacked pyrene-pyrene dimer of **1**, resulting in excimer fluorescence quenching. The fluorescent intensity ratio of monomer-to-excimer for **1** upon binding with ATP ( $I_{375}/I_{487}$ ) is much larger than that upon binding with ADP and AMP. This difference is large enough to discriminate ATP from ADP and AMP. As one of the biological applications, sensor **1** is successfully applied to the ATP staining experiments. Sensor **1** is also applied to monitor the hydrolysis of ATP and

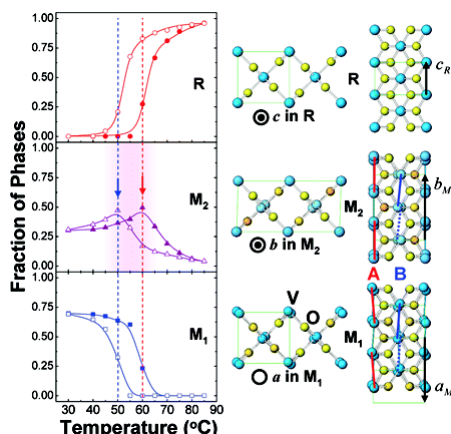




sections throughout the visible part of the solar spectrum turned out to be valuable in enhancing the overall light-harvesting features. Upon photoexcitation, for both SWNTs–ZnP 1 and 2, radical ion pair states (i.e., reduced SWNT and oxidized ZnP) are formed. The charge-separated states decay to regenerate the singlet ground state with lifetimes of 820 and 200 ps for 1 and 2, respectively.

- Surface-Stress-Induced Mott Transition and Nature of Associated Spatial Phase Transition in Single Crystalline VO<sub>2</sub> Nanowires  
Sohn, J. I.; Joo, H. J.; Ahn, D.; Lee, H. H.; Porter, A. E.; Kim, K.; Kang, D. J.; Welland, M. E. *Nano Lett.* **2009**, *9*, 3392–3397.

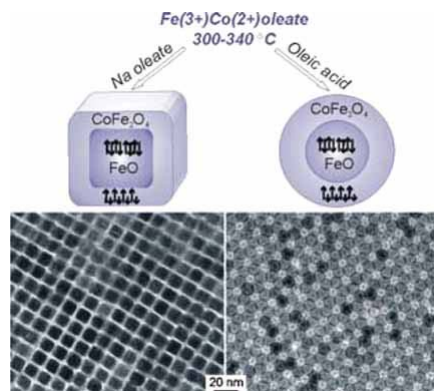
Abstract:



We demonstrate that the Mott metal–insulator transition (MIT) in single crystalline VO<sub>2</sub> nanowires is strongly mediated by surface stress as a consequence of the high surface area to volume ratio of individual nanowires. Further, we show that the stress-induced antiferromagnetic Mott insulating phase is critical in controlling the spatial extent and distribution of the insulating monoclinic and metallic rutile phases as well as the electrical characteristics of the Mott transition. This affords an understanding of the relationship between the structural phase transition and the Mott MIT.

- Exchange-Coupled Bimagnetic Wüstite/Metal Ferrite Core/Shell Nanocrystals: Size, Shape, and Compositional Control  
Bodnarchuk, M. I.; Kovalenko, M. V.; Groiss, H.; Resel, R.; Reissner, M.; Hesser, G.; Lechner, R. T.; Steiner, W.; Schäffler, F.; Heiss, W. *Small* **2009**, *5*, 2247 – 2252.

Abstract:



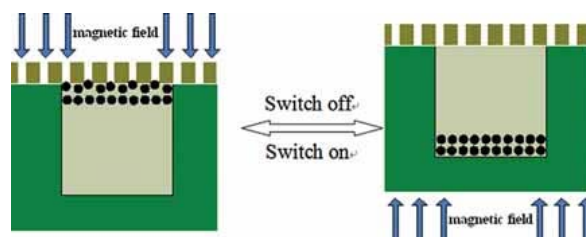
Iron oxide-based exchange-coupled nanomagnets consisting of antiferromagnetic wüstite (Fe<sub>x</sub>O) cores covered by ferrimagnetic metal ferrite shells (see figure) are chemically synthesized in a simple

one-pot procedure. The synthesis allows independent size, shape, and compositional control. The strong exchange coupling at the core/shell interface results in unique magnetic properties.

- Magnetically Triggered Reversible Controlled Drug Delivery from Microfabricated Polymeric Multireservoir Devices

Cai, K. Luo, Z.; Hu, Y.; Chen, X.; Liao, Y.; Yang, L.; Deng, L. *Adv. Mater.* **2009**, 4045-4049.

Abstract:

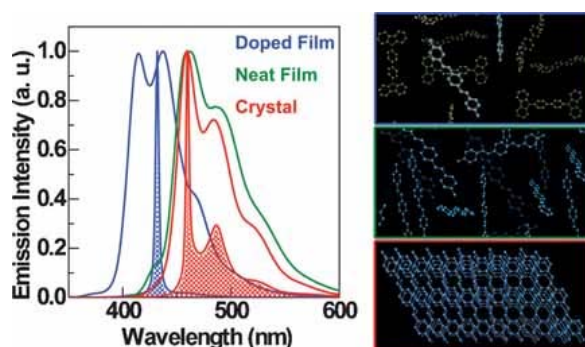


The pulsed reversible release of dual drugs from biodegradable polymeric multireservoir devices is successfully demonstrated. The controlled release is achieved by incorporating magnetic particles in the devices as switch carriers. It is possible to intentionally switch on/off the drug release at any desired time for a chosen duration.

- Effect of Molecular Morphology on Amplified Spontaneous Emission of Bis-Styrylbenzene Derivatives

Kabe, R.; Nakanotani, H.; Sakanoue, T.; Yahiro, M.; Adachi, C. *Adv. Mater.* **2009**, 4034-4038.

Abstract:



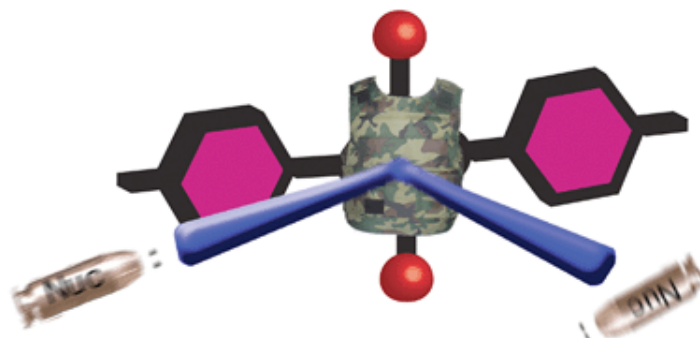
Molecular aggregation greatly affects the fluorescence quantum efficiency, transient lifetime, and amplified spontaneous emission (ASE) of bis-styrylbenzene derivatives. We compare the optical properties for various morphologies (solution, film, doped film, and single crystalline state) (see figure) and demonstrate that ambipolar operation of a 1,4-bis(4-methylstyryl) benzene layer in field-effect transistors leads to intense blue electroluminescence with a rather sharp emission width.

- Discovery and early development of squaraine rotaxanes.

Gassensmith, E. J.; Baumes, J. M.; Smith, B. D. *Chem. Commun.* **2009**, 6329 – 6338.

Abstract :

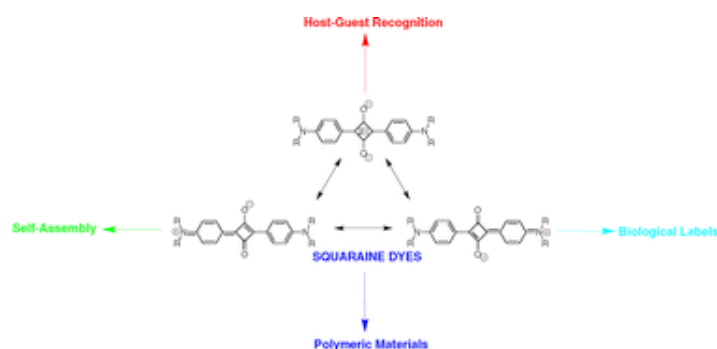




The chemical and photophysical properties of a fluorescent squaraine dye are greatly enhanced when it is mechanically encapsulated inside a tetralactam macrocycle. This feature article describes the synthesis, structure, and photophysical performance of first-generation squaraine rotaxanes, and shows how they can be used as fluorescent imaging probes and chemosensors.

- Squaraine dyes in molecular recognition and self-assembly.  
McEwen J. J.; Wallace, K. J. *Chem. Commun.* **2009**, 6339 – 6351.

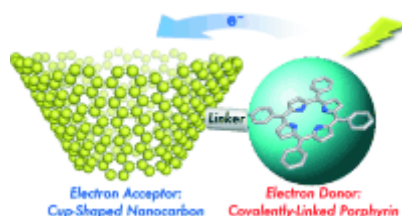
Abstract :



Squaraine dye molecules and their derivatives are gaining significant interest in the field of supramolecular chemistry, both in host–guest recognition and self-assembly. The unique structure and properties of squaraine molecules has led to extensive research into their use as sensors. This feature article covers the most recent studies (2004–2009) in the development, characterization, and application of squaraine dye-based molecular sensors, self-assembly, and their use in polymeric materials and biological applications.

- Synthesis, Characterization, Redox Properties, and Photodynamics of Donor–Acceptor Nanohybrids Composed of Size-Controlled Cup-Shaped Nanocarbons and Porphyrins  
Ohtani, M.; Saito, K.; Fukuzumi, S. *Chem. Eur. J.* **2009**, *15*, 9160-9168.

Abstract:



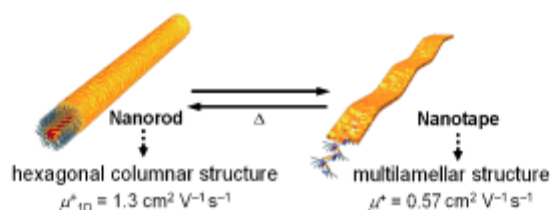
Cup-shaped nanocarbons (CNC) generated by the electron-transfer reduction of cup-stacked carbon nanotubes have been functionalized with porphyrins ( $H_2P$ ) as light-capturing chromophores. The resulting donor–acceptor nanohybrid has been characterized by thermogravimetric analysis (TGA), Raman and IR spectroscopy, transmission electron microscopy, elemental analysis, and UV/Vis

spectroscopy. The weight of the porphyrins attached to the cup-shaped nanocarbons was determined as 20% by TGA and elemental analysis. The UV/Vis absorption spectrum of CNC-(H<sub>2</sub>P)<sub>n</sub> in DMF agrees well with that obtained by the superposition of reference porphyrin (ref-H<sub>2</sub>P) and cupshaped nanocarbons. The photoexcitation of the CNC-(H<sub>2</sub>P)<sub>n</sub> nanohybrid results in formation of the charge-separated (CS) state to attain the longest CS lifetime (0.64±0.01 ms) ever reported for donor–acceptor nanohybrids, which may arise from efficient electron migration following the charge separation. The formation of a radical ion pair was detected directly by electron spin resonance (ESR) measurements under photoirradiation of CNC-(H<sub>2</sub>P)<sub>n</sub> with a high-pressure mercury lamp in frozen DMF at 153 K. The observed ESR signal at  $g = 2.0044$  agrees with that of ref-H<sub>2</sub>PC<sup>+</sup> produced by one-electron oxidation with [Ru(bpy)<sub>3</sub>]<sup>3+</sup> in deaerated CHCl<sub>3</sub>, indicating the formation of H<sub>2</sub>PC<sup>+</sup>. The electron-acceptor ability of the reference CNC compound (ref-CNC) was also examined by the electron-transfer reduction of ref-CNC by a series of semiquinone radical anions.

- Interconvertible Oligothiophene Nanorods and Nanotapes with High Charge-Carrier Mobilities

Yagai, S.; Kinoshita, T.; Kikkawa, Y.; Karatsu, T.; Kitamura, A.; Honsho, Y.; Seki, S. *Chem. Eur. J.* **2009**, *15*, 9320-9324.

Abstract:

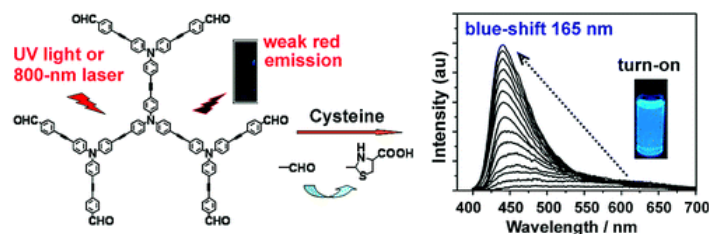


**Barbarian aggregates:** A barbituric acid-functionalized quarterthiophene self-aggregates in aliphatic solvents to form nanorods. Upon addition of a bismelamine receptor, the nanorods are converted into nanotapes, which can be thermally reconverted to nanorods. Nanorods and nanotapes self-organize into hexagonal columnar and multilamellar structures with high hole mobilities (see figure).

- One- and Two-Photon Turn-on Fluorescent Probe for Cysteine and Homocysteine with Large Emission Shift

Zhang, X.; Ren, X.; Xu, Q.-H.; Loh, K. P.; Chen, Z.-K. *Org. Lett.* **2009**, *11*, 1257–1260.

Abstract:

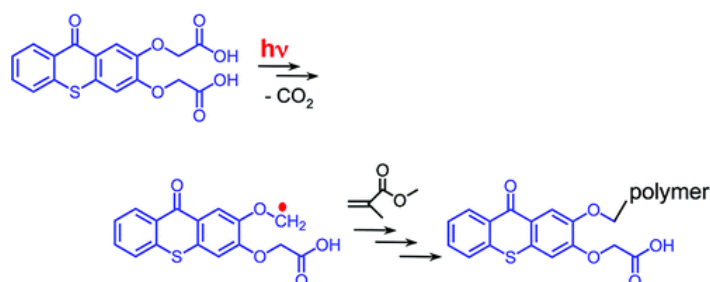


A novel dendritic chromophore with efficient intramolecular charge transfer (ICT) and strong two-photon absorption (TPA) was designed as a turn-on fluorescent probe for cysteine (Cys) and homocysteine (Hcy). The probe exhibited greatly enhanced fluorescence intensity as well as a very large emission peak shift (165 nm) upon addition of Cys/Hcy due to ICT switch off. The sensing process was also monitored by two-photon excited fluorescence (TPEF).

- Mechanistic Studies of Photoinitiated Free Radical Polymerization Using a Bifunctional Thioxanthone Acetic Acid Derivative as Photoinitiator.

Karasu, F.; Arsu, N.; Jockusch, S.; Turro, N.J. *Macromolecules* **2009**, *42*, 7318–7323.

Abstract:

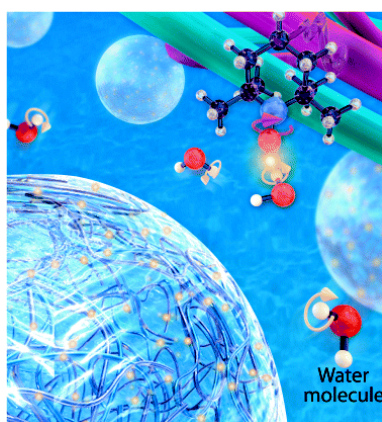


A bifunctional photoinitiator for free radical polymerization, thioxanthone catechol-O,O0-diacetic acid, was synthesized, characterized, and compared to photoinitiator parameters of the monofunctional analogue, 2-(carboxymethoxy)thioxanthone. Photophysical studies such as fluorescence, phosphorescence, and laser flash photolysis in addition to photopolymerizations of methyl methacrylate show that the bifunctional photoinitiator is more efficient in polymer generation than the monofunctional derivative. These studies suggest that initiator radicals are generated from a  $\pi$ - $\pi^*$  triplet state in an intramolecular electron transfer, followed by proton transfer and decarboxylation to generate alkyl radicals, which initiate polymerization. The initial electron transfer is faster for the bifunctional photoinitiator than the monofunctional derivative, which is based on laser flash photolysis studies. Because of the relatively fast intramolecular radical generation from the triplet state (triplet lifetime = 490 ns), quenching by molecular oxygen is insignificant and polymerization of methyl methacrylate proceeds efficiently without deoxygenation. At higher concentrations of initiator (~5 mM) intermolecular electron transfer competes with intramolecular electron transfer. Both processes, inter- and intramolecular processes, yield initiating alkyl radicals.

- Local Water Dynamics in Coacervated Polyelectrolytes Monitored through Dynamic Nuclear Polarization-Enhanced  $^1\text{H}$  NMR.

Kausik, R.; Srivastava, A.; Korevaar, P. A.; Stucky, G.; Waite, J. H.; Han, S. *Macromolecules* **2009**, *42*, 7404–7412.

Abstract:

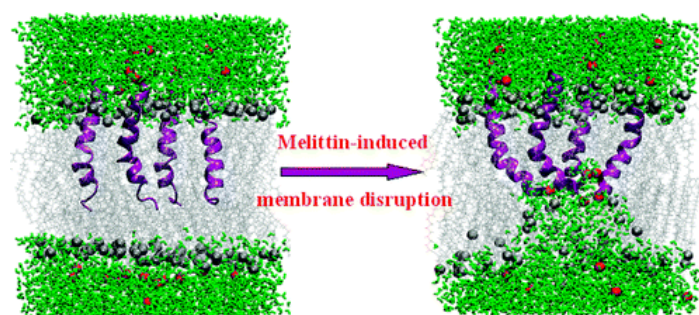


We present the first study of quantifying the diffusion coefficient of interfacial water on polyelectrolyte surfaces of systems fully dispersed in bulk water under ambient conditions. Such measurements were made possible through the implementation of a recently introduced dynamic

nuclear polarization (DNP) technique to selectively amplify the nuclear magnetic resonance (NMR) signal of hydration water that is interacting with specifically located spin-labels on polyelectrolyte surfaces. The merit of this novel capability is demonstrated in this report through the measurement of solvent microviscosity on the surface of two types of oppositely charged polyelectrolytes: when freely dissolved versus when complexed to form a liquid-liquid colloidal phase called complex coacervates. These complex coacervates were formed through electrostatic complexation between the imidazole-based cationic homopolymer poly(*N*-vinylimidazole) (PVIIm) and anionic polypeptide polyaspartate (PAsp) in the pH range of 4.5–6.0, under which conditions the coacervate droplets are highly fluidic yet densely packed with polyelectrolytes. We also investigated the rotational diffusion coefficients of the spin-labels covalently bound to the polyelectrolyte chains for both PVIIm and PAsp, showing a 5-fold change in the rotational correlation time as well as anisotropy parameter upon coacervation, which represents a surprisingly small decrease given the high polymer concentration inside the dense microdroplets. For both DNP and ESR experiments, the polymers were covalently tagged with stable nitroxide radical spin-labels (~1 wt %) to probe the local solvent and polymer segment dynamics. We found that the surface water diffusion coefficients near uncomplexed PVIIm and PAsp at pH 8 differ and are around  $D \sim 1.3 \times 10^{-9} \text{ m}^2/\text{s}$ . In contrast, inside the complex coacervate phase, the water diffusion coefficient in the immediate vicinity of either polyelectrolyte was  $D \sim 0.25 \times 10^{-9} \text{ m}^2/\text{s}$ , which is about an order of magnitude smaller than the bulk water self-diffusion coefficient and yet orders of magnitude greater than that of associated, bound, hydration water. This observation suggests the existence of measurable water inside complex coacervates with relatively high diffusion and exchange dynamics, implying that water moves in nanometer-scale pore spaces as opposed to being structurally bound or even absent. We infer from our observation that the PVIIm and PAsp chains are undergoing roughly pairwise association, so that largely charge-neutralized species compose the concentrated, yet fluidic, and partially hydrated coacervate cores.

- Cause and Effect of Melittin-Induced Pore Formation: A Computational Approach  
Manna, M.; Mukhopadhyay, C. *Langmuir* **2009**, *25*, 12235–12242.

Abstract:

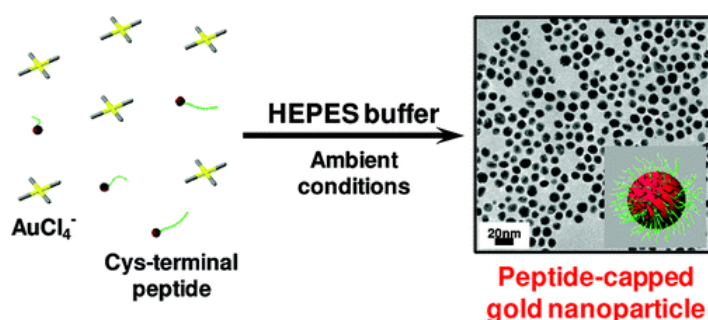


Melittin embedded in a palmitoyl oleyl phosphatidylcholine bilayer at a high peptide/lipid ratio (1:30) was simulated in the presence of explicit water and ions. The simulation results indicate the incipience of an ion-permeable water pore through collective membrane perturbation by bound peptides. The positively charged residues of melittin not only act as “anchors” but also disrupt the membrane, leading to cell lysis. A detailed analysis of the lipid tail order parameter profile depicts localized membrane perturbation. The lipids in the vicinity of the aqueous cavity adopt a tilted conformation, which allows local bilayer thinning. The prepore thus formed can be considered as the melittin-induced structural defects in the bilayer membrane. Because of the strong cationic nature, the melittin-induced prepore exhibits electivity toward anions over cations. As  $\text{Cl}^-$  ions entered into

the prepore, they are electrostatically entrapped by positively charged residues located at its wall. The confined motion of the Cl<sup>-</sup> ions in the membrane interior is obvious from calculated diffusion coefficients. Moreover, reorientation of the local lipids occurs in such a way that few lipid heads along with peptide helices can line the surface of the penetrating aqueous phase. The flipping of lipids argued in favor of melittin-induced toroidal pore over a barrel-stave mechanism. Thus, our result provides atomistic level details of the mechanism of membrane disruption by antimicrobial peptide melittin.

- Novel Synthetic Route to Peptide-Capped Gold Nanoparticles  
Serizawa, T.; Hirai, Y.; Aizawa, M. *Langmuir* **2009**, *25*, 12229–12234.

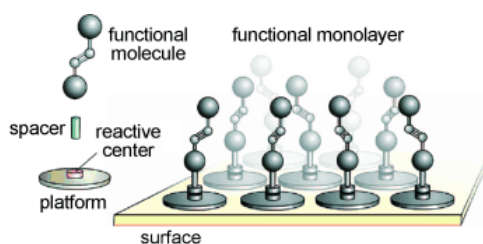
Abstract :



A novel synthetic route to peptide-capped gold nanoparticles was demonstrated herein. Tetrachloroaurate ions were reduced with 2-[4-(2-hydroxyethyl)-1-piperazinyl]ethanesulfonic acid (HEPES) under extremely mild conditions (pH 7.2, ambient temperature) in the presence of cysteine-terminal desired peptides, so that peptide-capped spherical nanoparticles were successfully synthesized. Model basic peptides containing the Arg-Pro-Thr-Arg sequence, which is an essential motif that specifically binds to film surfaces composed of isotactic poly(methyl methacrylate), were employed. Particle sizes were approximately 10 nm, and size distributions were narrow. Positive zeta potentials of nanoparticles suggested the presence of the Arg-Pro-Thr-Arg sequence on the outermost surface. Thermogravimetric analysis revealed that peptides were closely packed on the gold's surface. Parameters affecting reaction rates such as peptide structures and concentrations were investigated. Native peptide functions were conserved on nanoparticles by introducing a certain spacer between cysteine and the Arg-Pro-Thr-Arg sequence, suggesting that designing suitable peptide structures is essential to conserve peptide functions.

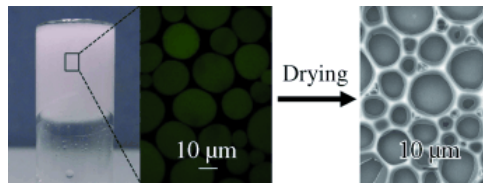
- Interfacial Systems Chemistry: Towards the Remote Control of Surface Properties  
Woll, C. *Angew. Chem. Int. Ed.* **2009**, *48*, 8406 – 8408.

Abstract:



**Flexible linkers:** Surface chemists have long strived to prepare surfaces with properties that can be adjusted by an external stimulus. In a new platform method a substrate-bound triacatriangulonium spacer provides the attached azobenzene molecule enough room so that it can change configurations upon irradiation (see picture).

- High Internal Phase Emulsions Stabilized Solely by Microgel Particles  
Li, Z.; Ming, T.; Wang, J.; Ngai, T. *Angew. Chem. Int. Ed.* **2009**, *48*, 8490–8493.  
Abstract:



**Smart microgels:** High internal phase emulsions (HIPEs) with a volume fraction up to 0.9 are prepared using soft microgel particles as stabilizer. Adsorption of microgels at the interface can effectively hinder droplet coalescence, and the excess particles form a gel in the continuous phase to inhibit creaming and phase inversion. Drying such HIPEs in air leads to porous materials.